MINUTIAE EXTRACTION SCHEME FOR FINGERPRINT RECOGNITION SYSTEMS

D. Simon-Zorita, J. Ortega-Garcia, S. Cruz-Llanas and J. Gonzalez-Rodriguez

Dpt. Ingenieria Audiovisual y Comunicaciones – Speech and Signal Processing Group (ATVS)
EUIT Telecomunicacion, Universidad Politecnica de Madrid, Spain
e-mail: dsimon@diac.upm.es; http://www.atvs.diac.upm.es

ABSTRACT

A complete minutiae extraction scheme for automatic fingerprint recognition systems is presented. The proposed method uses improving alternatives for the image enhancement process, leading consequently to an increase of the reliability in the minutiae extraction task. In the first stages, image normalization and orientation field of the fingerprint are calculated. The local orientation of the ridges will serve as parameter for the next processing stages. Details for the adaptive morphological filtering used to ridge extraction and background noise elimination are described. Evaluation results are obtained from both inked and scanned fingerprints. Conclusions in terms of *Goodness Index* (GI), which compares the results obtained by automatic minutiae extraction with manually extracted ones, are provided in order to test the global performance of this approach.

1. INTRODUCTION

One of the most important tasks considering an automatic fingerprint recognition system is the minutiae biometric pattern extraction from the captured image of the fingerprint [1]. In some cases, the fingerprint image comes from an inked fingerprint; in other cases, the image is obtained directly scanning the fingerprint. Due to imperfections of the acquired image, in some cases certain minutiae can be missed by the extraction algorithm, and in other cases spurious minutiae can be inserted [2,5]. Image imperfections can also generate errors in determining the coordinates of each true minutia and its relative orientation in the image. All these facts make remarkable decrease of the recognition system reliability, since fingerprint recognition is based on the comparison, within some tolerance limits, between the testing biometric pattern and the stored pattern. The algorithms developed and proposed in this paper for the image enhancement process have been tested with both inked and scanned fingerprints, leading to an evaluation of results in terms of *Goodness Index* (GI) [3,4], and allowing therefore a direct comparison between the automatically-extracted minutiae pattern and the pattern obtained by expert peer-inspection. Some conclusions regarding both image enhancement algorithms and GI results are also presented.

2. FINGERPRINT IMAGE ENHANCEMENT

To apply the proposed automatic minutiae extraction algorithmic solution, we have used fingerprints from the database DB 4 NIST Fingerprint Image Groups [6]. The NIST images derive from digitized inked fingerprints, each one consisting of 512x512 pixels, in 8-bit gray scale. The medium-quality of these inked fingerprints makes imperfections arise: non-uniformity of the ink density, appearance of non-printed areas, and also the existence of stains. The system has also been evaluated with scanned fingerprints, in which image brightness and contrast controls provide an increase of image quality, improving the computational efficiency of the global enhancement algorithm. The 100SC Precise Biometric fingerprint scanner has been used to acquire a small-sized fingerprint database (ATVS database), in order to compare the results with those obtained in the evaluation of the NIST fingerprints. ATVS database consists of 100 users with 300x300 pixel images, in 8-bit gray scale. Next, in order to accurately extract the minutiae of a fingerprint, the improved sequence of stages in which the complete outlined process consists is described.

2.1. Image normalization

The objective of this stage is to decrease the dynamic range of the gray scale between ridges and valleys of the image in order to facilitate the processing of the following stages. The normalization factor is calculated according to the mean and the variance of the image [3]. Figure 1 shows the original NIST "f05" image and the corresponding normalized fingerprint.

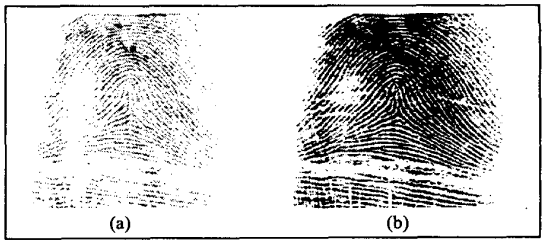

Figure 1: (a) NIST "f05" original image. (b) Normalized fingerprint.

0-7803-6725-1/01/$10.00 ©2001 IEEE

2.2. Calculation of the orientation field

The orientation field represents the local orientation of the ridges contained in the fingerprint. In order to estimate it, the image is divided in 16x16 pixel blocks and the gradient is calculated every pixel, in x and y coordinates. Due to the inherent computational load of the recognition process, it is enough to apply a mask of 3x3 pixels for the gradient calculation at each pixel. From the gradient information the orientation angle is estimated through the minimum square adjustment algorithm given in [1,3]. Often, in some blocks, the orientation angle is not correctly determined, due to background noise and ridges and valleys damages, caused by impression lacks of certain image areas. Therefore, as significant local angle variations between adjacent blocks cannot exist, a new spatial low-pass filtering is applied to the estimated oriented field to correctly re-align all the segments. The filter mask size used is 5x5 pixels, with fixed coefficient weighting of 1/25. Figure 2(a) shows the resulting orientation field obtained from gradient calculation. Figure 2(b) shows the re-aligned field obtained after the spatial low pass filtering. This orientation field will fix the adaptive filters parameters in successive stages.

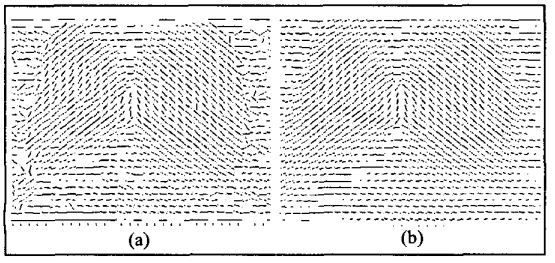

Figure 2: (a) Fingerprint oriented and (b) re-aligned fields.

2.3. Selection of the interest region

Since the image has background noise, the algorithm may generate minutiae outside the fingerprint area. To avoid this problem, the image area defined by all the 16x16 blocks, in which a high variance of the gray level in the normal direction of the ridges exists, is selected. Thus, the normal orientation field of the ridges is previously estimated. After that, the noisy area of the image, to be excluded in the following steps, is defined by low variance in all directions [4]. In figure 3 it is shown the variance for the NIST "f05" fingerprint and the interest region derived for subsequent stages.

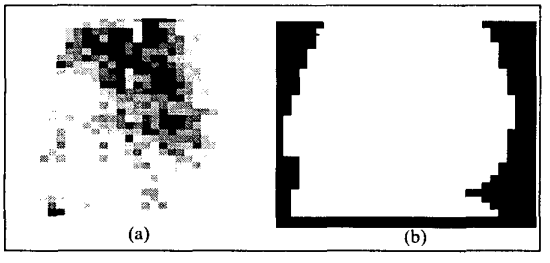

Figure 3: (a) Fingerprint variance and (b) interest region.

2.4. Ridge extraction

In order to decide whether a single pixel belongs or not to a given ridge, it is necessary to filter the fingerprint image with two adaptive masks, both capable to increase the gray level in the normal direction of the ridge [1]. The orientation of the mask is adapted within each 16x16 block, depending on the angles obtained from the orientation field of figure 2(b). If the gray level of a pixel exceeds a threshold in the two filtered images, it is thus considered that the pixel belongs to a ridge; otherwise, it is assigned to a valley, producing a binary image of the fingerprint. The dimensions of the mask are LxL (typ., L=5), and they are defined by the functions given in (1) and (2).

$$h_1(u,v)=\begin{cases}\dfrac{1}{\sqrt{2\pi}\,\delta}e^{-\left(\frac{u-u_0}{\delta}\right)^2}, \text{if}: u_0 = E[(v_c - v)c\,\mathrm{tg}(\theta)+u_c] \\ 0 \qquad\qquad \text{, otherwise}\end{cases} \tag{1}$$

$$h_2(u,v)=\begin{cases}\dfrac{1}{\sqrt{2\pi}\,\delta}e^{-\left(\frac{v-v_0}{\delta}\right)^2}, \text{if}: v_0 = E[(u_c - u)\mathrm{tg}(\theta)+v_c] \\ 0 \qquad\qquad \text{, otherwise}\end{cases} \tag{2}$$

$$\forall\, u, v \in [1, L]$$

where u and v are the coordinates of a pixel in the mask; (u_c,v_c), is the center of the mask; θ, is the orientation angle of the ridge in each image block, and δ, is a parameter to adjust the function mask to the width of the ridge. Figure 4(a) shows the filtered image with one of the spatial masks. Figure 4(b) represents the binary image obtained after a threshold is applied, producing smoother ridge borders.

For good quality fingerprint images, as in scanned fingerprints, the previous filtering process is simplified using just a single mask, with an spatially-oriented impulse (unit amplitude and zero width function), also spatially adapted to the angle of the ridges, and then also binaryzed through a threshold.

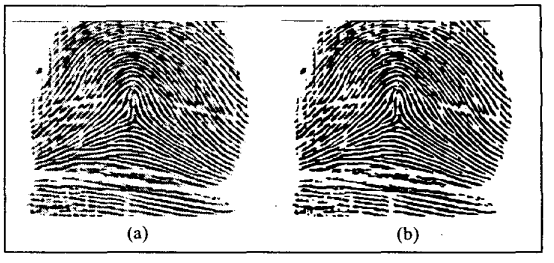

Figure 4: (a) Filtered image., (b) Obtained binary image.

2.5. Ridge profiling

To simplify the processing of the following steps, a new image filtering to profile the fingerprint ridges and eliminate the stains of certain areas is applied. In order to accomplish this process, the low frequency components are first extracted and then subtracted to the original image, providing the high frequency components necessary to profile the ridges, as can be derived from (3):

$$p[u,v] = f[u,v] + \lambda \cdot f_H[u,v] = f[u,v] + \lambda \cdot (f[u,v] - f_L[u,v]) \quad (3)$$

where $p[u,v]$, is the resulting profiling image; $f[u,v]$, is the binary image; $f_H[u,v]$ and $f_L[u,v]$ are, respectively, the high and low frequency images; and λ is a factor (λ>0), that determines the degree of profiling. In figure 5(a) the resulting filtered image is shown. An additional filtering can be applied to eliminate the spurious ridges due to stains in the image. Thus, a unit impulse mask is used, capable to locally adapt its orientation to the ridge orientation. The resulting binary image is shown in figure 5(b).

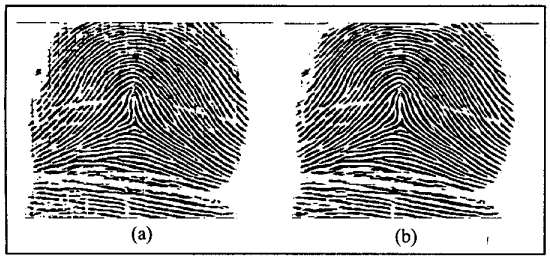

Figure 5: (a) Image after the first profiling filtering. (b) Image after the second profiling filtering with spatial mask.

2.6. Thinning

In this step two consecutive fast parallel thinning algorithms are applied, in order to reduce to a single pixel the width of the ridges in the binary image. These operations are necessary to simplify the subsequent structural analysis of the image for the extraction of the fingerprint minutiae. The thinning must be performed without modifying the original ridge structure of the image. During this process, the algorithms cannot miscalculate beginnings, endings and/or bifurcation of the ridges, neither ridges can be broken.

2.7. Imperfection removal

After thinning, depending on the image quality, the structural imperfections of the original fingerprint remain in certain degree. This results in breaking ridges, spurious ridges and holes; therefore, it is necessary to apply an algorithm for removing all the lines not corresponding to ridges and an algorithm to connect all the broken ridges. Figure 6(a) shows the thinned image obtained once the algorithms for thinning and imperfection removal are applied [2].

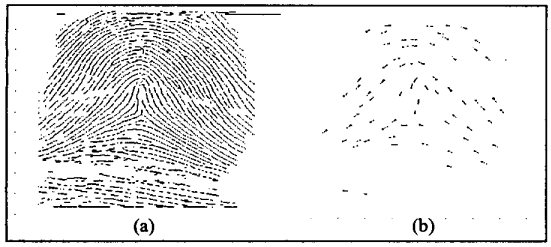

Figure 6: (a) Image after thinning and imperfection removal. (b) Minutiae pattern after cluster elimination process.

2.8. Minutiae extraction

In the last stage, the minutiae from the thinning image are extracted, obtaining accordingly the fingerprint biometric pattern. This process involves the determination of: *i*) whether a pixel, belongs to a ridge or not and, *ii*) if so, whether it is a bifurcation, a beginning or an ending point, obtaining thus a group of candidate minutiae. Next, all points at the border of the interest region are removed. Then, since the minutiae density per unit area cannot exceed a certain value, all the candidate-point clusters whose density exceed this value are substituted by a single minutia located at the center of the cluster. Figure 6(b) shows the resulting minutiae pattern. Once the minutiae extraction process is concluded, the resulting biometric pattern contains, typ., 70~80 points. Figure 7 shows the minutiae pattern obtained by the image enhancement algorithm superimposed on the normalized inked fingerprint image. Figure 8 represents, in a schematic way, a summary of the complete enhancement algorithm process for the minutiae extraction process described above.

Figure 7: Detected minutiae from NIST "f05" fingerprint.

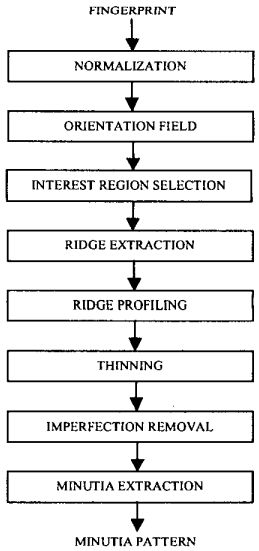

Figure 8: Complete image enhancement process.

Figure 9 shows an example of the minutiae patterns obtained by the image enhancement algorithm in the case of a scanned fingerprint.

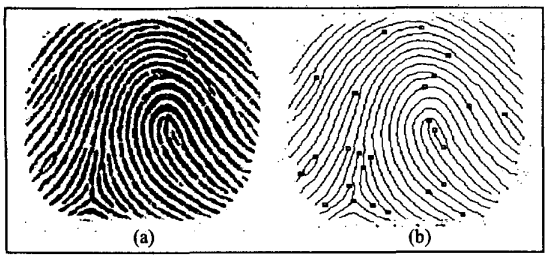

Figure 9: (a) Original fingerprint. (b) Detected minutiae.

3. EXPERIMENTAL RESULTS

As it is described in [3,4], matching of the minutiae pattern obtained by visual inspection with the minutiae pattern obtained by the automatic extraction algorithm is accomplished. In order to evaluate this process, the *Goodness Index* (GI) of the extracted minutiae is defined in (4) where an 8x8 pixel tolerance box to evaluate matching between the minutiae in the two patterns is considered:

$$GI = \frac{\sum_{i=1}^{r} q_i (p_i - d_i - i_i)}{\sum_{i=1}^{r} q_i t_i} \qquad (4)$$

where r, is the total number of 16x16 image blocks; p_i, is the number of minutiae paired in the ith block; d_i, is the number of deleted (missing) minutiae by the algorithm in the ith block; i_i, is the number of spurious inserted minutiae generated by the algorithm in the ith block; t_i, is the true number of minutiae in the ith block; and q_i, is a factor which represents the image quality in the ith block (good=4, medium=2, poor=1). A high value of GI indicates a high reliability degree of the extraction algorithm. The maximum value, GI=1, is reached when all true minutiae are detected and no spurious minutiae are generated. Table 1 presents both the GI values obtained with 10 inked medium-quality fingerprint images from the NIST database (left side), and also with 10 scanned high-quality fingerprint images from ATVS database (right side), allowing consequently to set in this last case the image-quality weighting factor q_i directly to 1. Nevertheless, in the NIST case, in order to determine the number of true minutiae, the previously proposed binary image skeleton has been used. Thus, the image-quality weighting factor q_i for NIST fingerprints has been also set to 1. Following this procedure, the total number of true minutiae vary within a range of 100 to 140 for NIST fingerprints, and 60 to 80 for ATVS ones, considering in both cases the entire interest region.

Under the experimental conditions mentioned above, the resulting values, in the case of both inked and scanned fingerprints, outperform those presented in [3,4]. As it is shown in table 1, the quoted GI values vary within a range of 0.24 to 0.61 for inked fingerprints, and 0.33 to 0.76 for scanned ones.

To probe the efficiency of the complete minutiae extraction algorithm we have matched, in a verification process, the minutiae biometric patterns obtained. The 100 users ATVS database employed contains both high and medium-quality fingerprints. Ten different images are acquired from each user to evaluate the false acceptance and false rejection curves. In this conditions the equal error rate obtained in a internal common mode is 4'28 %.

NIST	P	D	I	T	GI	ATVS	P	D	I	T	GI
f09	119	25	6	144	0.61	01	25	0	6	25	0.76
s04	100	11	22	111	0.60	02	45	5	5	50	0.70
s20	81	19	3	100	0.59	03	45	1	15	46	0.65
f05	91	23	4	114	0.56	04	48	8	7	56	0.59
s10	153	39	8	192	0.55	05	44	5	11	49	0.57
f18	77	29	0	103	0.45	06	45	8	8	53	0.55
s23	74	24	10	98	0.41	07	50	10	8	60	0.53
s16	105	40	7	145	0.40	08	46	5	18	51	0.45
f02	111	49	6	160	0.35	09	38	10	9	48	0.40
f12	117	46	31	163	0.24	10	29	1	18	30	0.33

Table 1: GI values for NIST and ATVS fingerprints. P stands for "paired"; D, "deleted"; I, "inserted"; T, "true" minutiae.

4. CONCLUSIONS

The reliability of any automatic fingerprint recognition system strongly relies on the precision obtained in the minutiae extraction process. The complete image enhancement process proposed has been tested on a group of 10 inked medium-quality fingerprint images and 10 scanned ones, in order to evaluate its reliability in terms of image enhancement determined by the GI. Several relevant contributions have been proposed in this paper: *i)* the image enhancing process through the local oriented filtering of the image with two adaptive masks in order to extract the ridges of the fingerprint, *ii)* the reliable extraction of the ridge orientation angle through a previous re-estimate of the calculated orientation field, *iii)* the filtering process with a single adaptive mask of pulses in the case of scanned fingerprints and, *iv)* the ridge profile process, mainly in the case of inked fingerprints, since its skeleton is better defined, reducing the size of the possible stains of the image. A more precise minutiae localization process has been implemented, reducing consequently the generation of spurious inserted minutiae. The consistent improvements found in the global image enhancement process lead to relatively high GI values, resulting in a competitive scheme compared to those previously proposed.

5 REFERENCES

[1] A. Jain, L. Hong and R. Bolle, "On-Line Fingerprint Verification", IEEE Trans. Pattern Analysis and Machine Intelligence, Vol.19, No.4, pp. 302-314, Apr. 1997.

[2] D.C. Douglas Hung, "Enhancement and Feature Purification of Fingerprint Images", Pattern Recognition, Vol. 26, No. 11, pp. 1661-1671, Nov. 1993.

[3] L. Hong, Y. Wan, and A. Jain, "Fingerprint Image Enhancement: Algorithm and Performance Evaluation", IEEE Trans. Pattern Analysis and Machine Intelligence, Vol. 20, No. 8, pp. 777-789, Aug. 1998.

[4] N. K. Ratha, S. Chen, and A. Jain, "Adaptive Flow Orientation-Based Feature Extraction in Fingerprint Images", Pattern Recognition, Vol. 28, No. 11, pp. 1657-1672, Nov. 1995.

[5] N. Ratha, K. Karu, S. Chen, and A. Jain, "A Real Time Matching System for Large Fingerprint Databases", IEEE Trans. on Pattern Analysis and Machine Intelligence, Vol. 18, No. 8, pp. 799-813, Aug. 1996.

[6] http://www.nist.gov